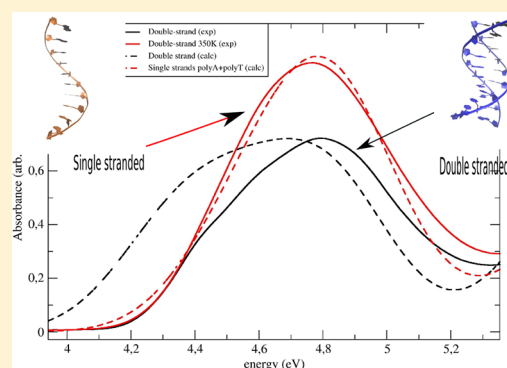


On the Nature of DNA Hyperchromic Effect

Marco D'Abramo,^{*,†} Chiara Lara Castellazzi,[‡] Modesto Orozco,^{‡,§,||} and Andrea Amadei^{*,⊥}[†]CINECA - Roma, via dei Tizii, 6, 00185, Roma, Italy[‡]Institute for Research in Biomedicine (IRB Barcelona), Barcelona, Spain[§]Joint IRB-BSC Program in Computational Biology, Barcelona, Spain^{||}Department of Biochemistry and Molecular Biology, University of Barcelona, Barcelona, Spain[⊥]Dipartimento di Scienze e Tecnologie Chimiche, Università di Roma, Tor Vergata, via della Ricerca Scientifica 1, 00133 Roma, Italy

S Supporting Information

ABSTRACT: A combined theoretical–experimental study of the hyperchromic effect as occurring in the denaturation of a double stranded polyA-polyT is presented. Our theoretical/computational procedure allows us to reproduce the essential features of the experimental spectra and to characterize those molecular interactions responsible for the changes in the UV absorbance. We found that although excitonic intrastrand interactions strongly affect the absorbance, they are almost fully maintained in the single-stranded DNA. Our data indicate that hyperchromic effect originates from the higher delocalization of the excitonic states in the denaturated DNA with respect to the double-stranded conformation.



INTRODUCTION

Because of its unique chemistry and structure, DNA shows very peculiar electronic properties. A complete understanding of these properties at an atomic-molecular point of view is crucial to shed light on several fundamental biophysical–biochemical processes occurring in living organism,^{1,2} to improve DNA sequencing,³ to detect somatic mutations,⁴ and to enhance emerging therapeutic strategies.⁵

Among others, the so-called hyperchromic effect, which refers to the experimentally observed change in absorbance after DNA denaturation, is a very important property of DNA. This effect is routinely used to record melting curves by monitoring the change in absorbance when the DNA undergoes a conformational transition from double-stranded to single-stranded structure in response to a chemical or physical perturbation. On a physical–chemistry ground, such an effect is determined by the DNA excited-wave function, which is spatially delocalized along the molecule, and thus it is different from the simple recombination of the single nucleobase monomeric electronic wave functions.

Although recent experiments have elucidated the role of the DNA interactions on the fate of the excited states,⁶ the nature of the hyperchromism in DNA still remains elusive,⁷ mainly because it is hard to characterize the excited state spatial delocalization and the mechanism leading to the hyperchromism in terms of molecular interactions.^{8–10} From a theoretical viewpoint, a detailed description of the electronic degrees of freedom involved in the process coupled to an exhaustive and rigorous treatment of the molecular config-

urations needed to reproduce the experimental behavior still represents a challenge. Thus, the large majority of the theoretical studies deals with an “averaged” description of the environmental effects or with a reduced sampling of the conformational space.^{11–15} Despite the different theoretical/computational approaches used, all of these works pointed out that a proper description of the delocalization of the nucleobase excited states is required to model the UV-absorption properties of single- and double-stranded DNA molecules.

However, the usual approaches are necessarily based on relevant approximations to make the calculation feasible. The use of *ab initio* calculations for the whole oligomer avoids high-level treatment of the electronic states and necessarily requires the use of rather simplified molecular models¹² (i.e., only dimer and trimer single-stranded conditions). The use of excitonic theory – based on modeling the oligomer excited states via combinations of the monomers states – allows the use of high-level *ab initio* calculations and more realistic molecular models (including single- and double-stranded DNA molecules). However, these latter approaches are typically lacking a proper atomistic-level treatment of the environmental perturbation effects and describe the chromophores interaction only by using their mutual excitonic coupling,^{11,16} being unable to treat charge-transfer states.

Received: April 5, 2013

Revised: June 18, 2013

Published: June 25, 2013



We report here on the application of a mixed Molecular-Mechanics–Quantum-Mechanical approach – the perturbed matrix method (PMM)^{17–19} – which is able to reproduce the hyperchromic shift occurring in the denaturation of the DNA decamer polyA–polyT by coupling all-atoms molecular dynamics simulations of DNA with an accurate theoretical description of the electronic properties of the nucleobases. The method presented allows us to rigorously treat the electronic coupling between neighboring bases within a robust statistical mechanical framework, and thus it is able to gain insight into the intra- and interstrand interactions between DNA bases, which ultimately determine the UV spectrum. Note that in the present approach the subpart of the system treated at a quantum-mechanical level (the quantum centers (QCs)) is defined by virtually all of the base pairs of the DNA molecule, including all of the environmental perturbative effects in the calculations.

Therefore, within our approach,¹⁹ not only are all of the environmental perturbations explicitly included at an atomistic level of detail but also all of the chromophores interactions are treated, beyond the use of the excitonic coupling, by considering the mutual perturbation effects due to the chromophore atomic charges (i.e., each chromophore is perturbed by the electric field due to the environment and to the other chromophores' ground-state atomic charges). In our methodology the reference electronic basis set is built by combining the perturbed single chromophore electronic excited states, which hence already include environmental and (ground-state) chromophore atomic charges interactions. This is a relevant difference with usual approaches,^{11,16,20} which construct the reference basis set by using the gas-phase single chromophores electronic states (i.e., unperturbed chromophores states). Finally, by means of diagonalization of the excitonic matrix,¹⁹ we obtain the excitonic coupling using the dipolar approximation¹¹ to describe the chromophores interaction operator. Such an approach typically allows an accurate treatment of the electronic excited states in interacting chromophores, as shown in the case of the water dimer, where it well-reproduced the first and second excitation energy shifts with respect to the monomer, as obtained by means of high-level *ab initio* calculations. (See table 1 of ref 19 and references therein.) Treatment of charge-transfer states, although, in principle, possible,²¹ is not considered here because it requires a further development of the theory involving relevant complications and it goes beyond the scope of the present work. However, theoretical results on similar systems (i.e., methyladenine) suggest that only a limited charge redistribution is associated with the electronic states responsible for the UV absorption spectrum. (See table 1 in Santoro et al.¹²)

Comparing the results of the calculations with the experimental UV absorption spectrum, we show that it is possible not only to reproduce the essential features of the hyperchromic effect but also to rationalize its nature on a chemical–physics ground. Our analysis of the excitonic effects in DNA strongly suggests that the deletion of the pairing interactions causes the increase in the absorbance observed in DNA denaturation experiments, as a result of the intrastrand excitonic coupling, which is almost fully maintained in the single-stranded DNA at high temperature (350 K). To the best of our knowledge, the present work is the first theoretical characterization of the UV spectrum of a DNA molecule at different temperatures, which is able to quantitatively reproduce and explain the experimentally observed hyperchromic effect.

METHODS

THEORY

Basic Derivations. Defining with \mathbf{r}_n the nuclear coordinates of the QC and \mathbf{x} the coordinates of the atoms providing the (classical) perturbing field, we can write the QC (electronic) Hamiltonian matrix (i.e., the matrix expressing the Hamiltonian operator) as^{18,19}

$$\begin{aligned}\tilde{H} &= \tilde{H}^0(\mathbf{r}_n) + \tilde{V}(\mathbf{r}_0, \mathbf{x}) \\ &\cong \tilde{H}^0(\mathbf{r}_n) + q_T \mathcal{V}(\mathbf{r}_0, \mathbf{x}) \tilde{I} + \tilde{Z}_1(\mathbf{E}(\mathbf{r}_0, \mathbf{x}), \mathbf{r}_n) \\ &\quad + \Delta V(\mathbf{r}_n, \mathbf{x}) \tilde{I}\end{aligned}\quad (1)$$

where \tilde{H}^0 is the QC unperturbed Hamiltonian matrix, \tilde{V} is the perturbation matrix, q_T is the QC total charge, $\mathcal{V}(\mathbf{r}_0, \mathbf{x})$ and $\mathbf{E}(\mathbf{r}_0, \mathbf{x})$ are the (perturbing) electric potential and electric field, as provided by the environment atomic charges, at a given QC \mathbf{r}_0 position (typically the mass center), $\tilde{Z}_1(\mathbf{E}, \mathbf{r}_n)$ is the perturbation energy matrix explicitly given by $[\tilde{Z}_1]_{ll'} = -\mathbf{E} \cdot \langle \Phi_l^0 | \hat{\boldsymbol{\mu}} | \Phi_{l'}^0 \rangle$ where $\hat{\boldsymbol{\mu}}$ is the dipole operator, \tilde{I} is the identity matrix, and $\Delta V(\mathbf{r}_n, \mathbf{x})$ approximates all of the higher order terms as a short-range potential. (Note that in the case the QC is a subpart of a molecule ΔV may also include an additive constant corresponding to a possible reference energy shift.) The previous equation providing the QC perturbed Hamiltonian matrix \tilde{H} for a QC interacting with a semiclassical atomic-molecular environment may be equivalently expressed in the typical operator notation

$$\begin{aligned}\hat{H} &= \hat{H}^0 + \hat{V} \\ &\cong \hat{H}^0 + q_T \mathcal{V} - \mathbf{E} \cdot \hat{\boldsymbol{\mu}} + \Delta V\end{aligned}\quad (2)$$

with the perturbation operator \hat{V} physically corresponding to the perturbation due to the ground-state environment atomic-molecular field acting on the QC. The eigenvectors of \hat{H} , that is, the eigenstates of \hat{H} , can be used to obtain the perturbed QC electronic properties for each QC perturbed state at each atomic configuration as provided by any sampling method, for example, MD simulations.

Extension to Interacting Chromophores. The relations derived in the previous subsection may be used to treat any quantum process of a chemical system (the QC) embedded into a semiclassical environment (i.e., we may assume factorization of the overall wave function and invariance of the environment electronic ground state for QC state transitions). In case we deal with a set of N interacting chromophores (N QCs) embedded in a semiclassical molecular environment, it is clear that we must take into account the possible excitation coupling occurring between QCs, partially breaking the previous approximations. In such a case, we can still assume that the overall electronic ground state may be defined by the product of QCs and environment ground states. However, excited-state factorization and QC independent excitations cannot be simply assumed. Therefore, we extended our previous results to treat such a condition by considering the perturbed Hamiltonian operator for all of the N QCs. The mathematical derivations (details discussed in our previous paper¹⁹) lead to describe the perturbed Hamiltonian matrix \tilde{H} by

$$\tilde{H} = \varepsilon_0 \tilde{I} + \Delta \tilde{H} \quad (3)$$

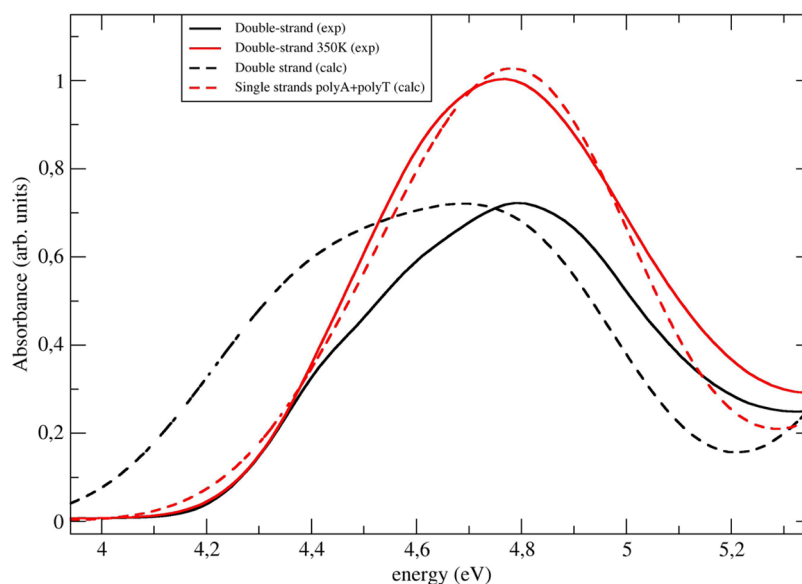


Figure 1. Theoretical and experimental absorption spectra of DNA at different temperatures.

where ε_0 is the electronic ground-state energy, and $\Delta\tilde{H}$ (excitation matrix) has the first row and column defined by null elements with its diagonal elements (beyond the null ground state one) given by the single chromophores perturbed excitation energies. Furthermore, via multipolar expansion (truncated at dipolar terms) of the chromophore interaction operator, the excitation matrix nonzero off-diagonal elements (in a.u.) are given by

$$\hat{V}_{k,k'} \cong \frac{q_{T,k}q_{T,k'}}{R_{k,k'}} + \frac{q_{T,k}\hat{\mu}_{k'}\cdot\mathbf{R}_{k,k'}}{R_{k,k'}^3} - \frac{q_{T,k'}\hat{\mu}_k\cdot\mathbf{R}_{k,k'}}{R_{k,k'}^3} + \frac{\hat{\mu}_k\cdot\hat{\mu}_{k'}}{R_{k,k'}^3} - 3\frac{\hat{\mu}_{k'}\cdot\mathbf{R}_{k,k'}\hat{\mu}_k\cdot\mathbf{R}_{k,k'}}{R_{k,k'}^5} \quad (4)$$

where $\hat{\mu}_k$ is the k th chromophore dipole operator and $\mathbf{R}_{k,k'}$ is the k' to k chromophore displacement vector defined by the corresponding chromophore origins (typically the centers of mass or geometry).

Note that from eq 3 it is evident that the excitation matrix provides the eigenvectors of \tilde{H} with eigenvalues corresponding to the N QCs excitation energies.

Using the same reference basis set, we may obtain the dipole matrix elements from the definition of the N QCs dipole operator¹⁹ $\hat{\mu}$

$$\hat{\mu} = \sum_l \hat{\mu}_l + \sum_l q_{T,l}\mathbf{R}_l \quad (5)$$

($\hat{\mu}$ is the l th chromophore dipole operator with respect to the l th chromophore origin and \mathbf{R}_l the vector radius defining the l th origin position in the laboratory reference of frame.)

■ EXPERIMENTAL AND COMPUTATIONAL METHODS

Computational Methods. The geometry of the double-stranded (polyA-polyT) DNA was generated as a canonical B-DNA double-helix structure using the 3DNA software package.²² The two strands were used as the starting structure for the simulations of the single-stranded polyA and polyT. The structures were minimized, solvated, neutralized, and then equilibrated for 10 ns using the BSC0 force field.²³ Three

isothermal–isobaric (NPT) MD simulations of 75 ns (ds) at 300 K and 100 ns (polyA and polyT) at 350 K were performed using the Gromacs software package²⁴ with a time step of 2 fs. Temperature and pressure were kept constant using the velocity-rescaling algorithm²⁵ and the Parrinello–Rahman barostat,²⁶ respectively. The PME method²⁷ was used to treat the long-range electrostatic interactions (cutoff 1.2 nm). The electronic calculations were performed using the MOLPRO software.²⁸ The geometries of adenine and thymine were minimized using the density functional theory (B3LYP functional) and the aug-cc-pvdz basis set. The transition dipole matrices between ground and the first three excited states (needed to apply the perturbed matrix method) were obtained by means of the CASSCF method^{29,30} (10 electrons in 12 orbitals). The energies of the electronic states were computed applying the CASPT2 method^{31,32} on the electronic wave function obtained by the CASSCF procedure. The IPEA shift procedure³³ ($\varepsilon = 0.2$) as implemented in MOLPRO was used to address the intruder state problem. These unperturbed properties are in line with experimental results and previous quantum-mechanical calculations. (See Table S1 in Supporting Information.) The electronic states were then perturbed using the electric field trajectory obtained from the molecular dynamics simulations within the PMM framework,^{34–36} and the corresponding perturbed properties were obtained, thus allowing the calculation of the spectral signal (the molecular extinction coefficient). Although the adenine and thymine geometries sampled along the molecular dynamics simulations did not show any relevant structural change from the ab initio optimized geometries (data not shown), such small structural fluctuations were included in the spectral signals by means of using for each single MD frame absorption a Gaussian probability distribution providing the vibrational effects when considering semiclassical vibrational states. Note that the variance of the Gaussian distribution (corresponding to 0.001 hartree) was explicitly evaluated by ab initio calculations performed on a set of MD-sampled chromophore geometries and, hence, no adjustable parameters were used in the calculation of the spectra.

Table 1. Values and Position of the Absorption Maximum Calculated for Different Sets of Quantum Centers^a

num	mol	T (K)	QC	abs. max	energy max. (eV)	interactions
1	DS	300	Ade5-Thy16	4.6	4.55	pairing
2	DS	300	Ade5:6-Thy15:16	3.5	4.80	stacking+pairing
3	DS	300	Ade4:5:6-Thy15:16:17	2.8	4.80–4.85	stacking+pairing
4	DS	300	Ade4:5:6:7-Thy14:15:16:17	2.8	4.85	stacking+pairing
5	DS	300	Ade3:4:5:6:7-Thy14:15:16:17:18	3.0	4.85	stacking+pairing
6	DS	300	Ade4:5:6:7	3.8	4.45	stacking
7	DS	300	Thy14:15:16:17	3.8	4.85	stacking
8	DS	300	Ade4:5:6	4.1	4.50	stacking
9	D	300	Thy15:16:17	3.85	4.85	stacking
10	DS	300	Ade5:6	4.8	4.75	stacking
11	DS	300	Thy15:16	4.05	4.80	stacking
12	DS	300	Ade5	10.5	4.80	none
13	DS	300	Thy16	4.25	4.75	none
14	DS	300	Ade5+Thy16	7.15	4.75	none
15	DS	300	Ade5:6+Thy15:16	4.2	4.80	stacking
16	DS	300	Ade4:5:6+Thy15:16:17	3.5	4.85	stacking
17	DS	300	Ade4:5:6:7+Thy14:15:16:17	3.5	4.85	stacking
18	SS	350	Ade5	7.7	4.75	none
19	SS	350	Ade4:5	7.5	4.80	stacking
20	SS	350	Ade4:5:6	4.8	4.85	stacking
21	SS	350	Ade4:5:6:7	4.8	4.85	stacking
22	SS	350	Ade3:4:5:6:7	4.4	4.85	stacking
23	SS	350	Thy5	3.6	4.80	none
24	SS	350	Thy5:6	3.3	4.75	stacking
25	SS	350	Thy4:5:6	3.3	4.80	stacking
26	SS	350	Thy4:5:6:7	3.0	4.80	stacking
27	SS	350	Ade4:5:6+Thy4:5:6	3.8	4.85	stacking

^aQCs column describes the quantum centers definition. The minus sign indicates that all of the nucleobases are included in the interacting QCs and hence involved in the excitonic calculations; the plus sign indicates that the value is obtained considering two sets of interacting QCs separately, hence with no excitonic coupling between the sets and then the corresponding spectra summed.

Experimental Methods. The oligonucleotides (a polyA and a polyT of 20 base pairs) were synthesized and purified by Sigma-Aldrich. Complementary strands were heated to 85 °C for 5 min in cacodylate buffer pH 6.5 (10 mM sodium cacodylate, 100 mM sodium chloride, 10 mM magnesium chloride) at a concentration of 1,5 M. The temperature was slowly decreased until room temperature to favor the annealing between the two strands. The UV spectrum of polyA–polyT duplex was obtained with a Jasco V650 spectrophotometer reading the absorbance of the sample at different wavelengths (from 230 to 320 nm) and temperatures (300 and 350 K).

RESULTS AND DISCUSSION

In Figure 1, we compare the theoretical spectra of the double- and single-stranded DNA with the corresponding experimental spectra. From the theoretical spectrum of the double-stranded DNA at 300 K and that obtained by summing the two spectra of the single-stranded polyA and polyT at 350 K we estimated that the melting of DNA induces an increase in the absorbance maximum of ~30% and a slight red shift. (The spectra relative noise is ~5%.) These results are in good agreement with the experimental counterparts, which provide essentially the same frequency for the spectra maxima and an increase of the absorbance of ~30% when DNA is heated (Figure 1). Interestingly, the calculated spectra also reproduce reasonably well the experimental spectra widths and shapes, although the calculated spectrum at 300 K is slightly shifted and, in the low energy tail, overestimated with respect to the experimental one.

(This is probably due to the inaccuracies of the ab initio calculations providing the unperturbed properties.)

Notwithstanding, our most relevant findings come out from the analysis of the DNA intramolecular and intermolecular interactions reported in Table 1, obtained by systematically removing interstrand or intrastrand excitonic interactions in our calculations to elucidate their contributions to the absorbance change.

First, our data point out that the presence of both interstrand and intrastrand excitonic interactions causes a decrease in the absorbance maximum, which is significantly larger in the case of adenines with respect to thymines (Table 1).

Focusing on the effects due to only including pairing interactions in the double-stranded DNA excitonic coupling, it follows that the absorbance maximum is insensitive to the number of base-pairs included in the QCs, beyond a single pair. This is clear by comparing the difference in the absorbance maximum of the spectra obtained considering all the interactions (sets 2, 3, and 4 of Table 1) with those where pairing interactions have been removed (sets 15, 16, and 17 of Table 1). Such a difference, in fact, remains constant for an increasing number of bases involved in the electronic coupling (set 2 vs 15, set 3 vs 16, set 4 vs 17).

The theoretical description of the intrastrand (stacking) interactions requires that at least three bases should be included in the excitonic coupling or, in other words, that the excitonic state responsible for the UV-spectrum is delocalized on three stacked bases. In fact, the value of the absorbance maximum decreases monotonically going from QCs formed by one to

three bases (Figure S1 in the Supporting Information) but remains practically constant when including one or two additional bases. (See Table 1.) Recent experimental works, based on the analysis of the transient absorption signals^{8,9} and of the CD spectrum¹⁰ of adenine oligonucleotides, suggested that the extent of the DNA electronic delocalization includes two to three nucleobases, in line with our results.

The other major finding of our work, which allows us to explain the DNA hyperchromic effect, is that the decrease in the absorbance due to the intrastrand interactions is practically the same in the double- and in the single-stranded DNA. Therefore, the absorbance difference between single- and double-stranded DNA, which causes the experimentally observed hyperchromic effect, should be due to the lack of pairing interactions in the single-stranded conditions. Such a result is in agreement with the above-mentioned experimental works,^{8,10} where it was demonstrated that delocalized excitonic states are present in DNA single-stranded homoadenine sequences of similar length (about 10 bases) to the molecule used in this paper.

The results summarized in Table 1 clearly point out that the use of QCs formed by either three bases (single-stranded DNA) or three base pairs (double-stranded DNA) can be used as the proper smallest set of chromophores providing accurate information on the DNA absorption behavior. Therefore, in the following, all of the data and analysis reported were obtained using such minimal QCs set.

To characterize in detail the DNA electronic properties in the presence and in the absence of the pairing excitonic interactions, which, based on our results, cause the hyperchromic effect, we have analyzed the perturbed electronic eigenstates relevant for the DNA absorption discussed above.

We found that in the frequency window of interest three perturbed electronic eigenstates (10th, 11th, and 12th excited states) give the major contribution to the absorption spectrum of the double-stranded DNA (Figure S2 in the Supporting Information), while the spectra of the single-stranded molecules are described almost completely by a few of the first excited eigenstates (Figure S3 in the Supporting Information).

We have characterized the essential features of such electronic eigenstates in terms of single nucleobases electronic states and properties. Concerning the double-stranded DNA (ds-DNA), the 12th excited eigenstate corresponds to the mixing of the single base second excited states of the three thymines, whereas the 10th and 11th excited eigenstates are almost completely defined by single base adenine excited states mixing. Therefore, the absence of mixing between thymine and adenine excited states in the ds-DNA strongly suggests that the observed hyperchromic effect must be due to a different intrastrand mixing of the single-base excited states induced by deletion of the excitonic pairing interactions.

To gain insight into this matter, we describe the degree of the excited eigenstate delocalization by the property s defined as $s = 1 - p_{\max}$ where p_{\max} represents the highest single base square projection of the chosen excitonic eigenstate. (The variable s thus provides a measure of the probability to involve the other single bases.)

The distributions of the s value for the relevant eigenstates of the ss-DNA at 350 K and the ds-DNA at 300 K in both the absence and presence of pairing interactions are reported in Figures 2 and 3. The effect of both pairing interaction and temperature increase is to remarkably reduce the degree of

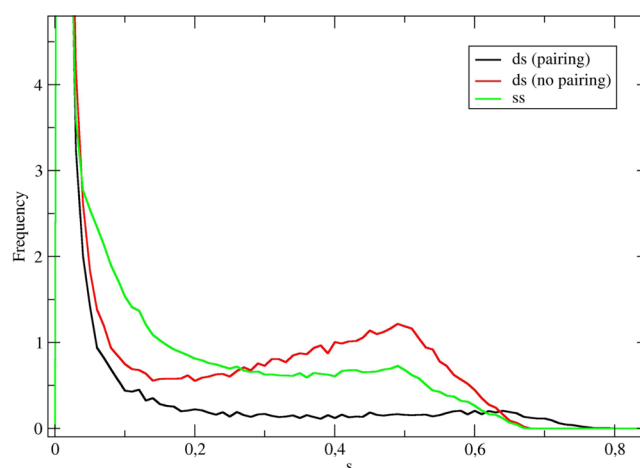


Figure 2. Distributions of the s values for the most important eigenstates of adenines: eigenstates 10 and 11 (ds-DNA at 300 K, six nucleobases as QCs, black line), eigenstates 4, 5, and 6 (ds-DNA at 300 K, three adenines as QCs, red line), and eigenstates 4, 5, and 6 (ss-DNA at 350 K, three adenines as QCs, green line). For the sake of clarity, when the distribution describes two or more eigenstates, only the mean distribution is reported.

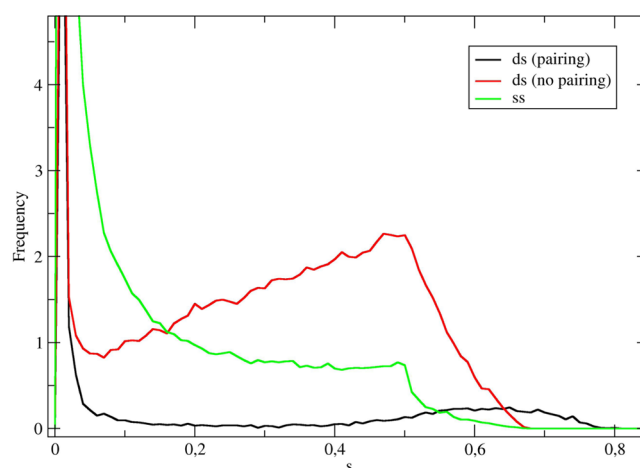


Figure 3. Distributions of the s values for the most important eigenstates of thymines: eigenstates 12 (ds-DNA at 300 K, six nucleobases as QCs, black line), eigenstates 4, 5, and 6 (ds-DNA at 300 K, three thymines as QCs, red line), and eigenstates 4, 5, and 6 (ss-DNA at 350 K, three thymines as QCs, green line). For the sake of clarity, when the distribution describes two or more eigenstates, only the mean distribution is reported.

delocalization of the excitonic states. However, the former is more pronounced, and hence the DNA denaturation results in an increase in delocalization (i.e., the excitonic coupling). Therefore, our data indicate that the increase in the absorbance maximum associated with the DNA denaturation, that is, the hyperchromism, is due to a higher delocalization of the ss-DNA excitonic states involved in the electronic transitions occurring between 4.7 and 4.9 eV.

The possibility that the ss-DNA simulations are not long enough to allow a sufficient sampling of their conformational spaces, that is, the sampling is affected by the starting (stacked) conditions, was investigated by comparing the distribution of the DNA helical parameters with the corresponding value for the ideal B-DNA. From such distributions (Figures 4 and 5) it comes out that the ss-DNAs explore a range of values of the

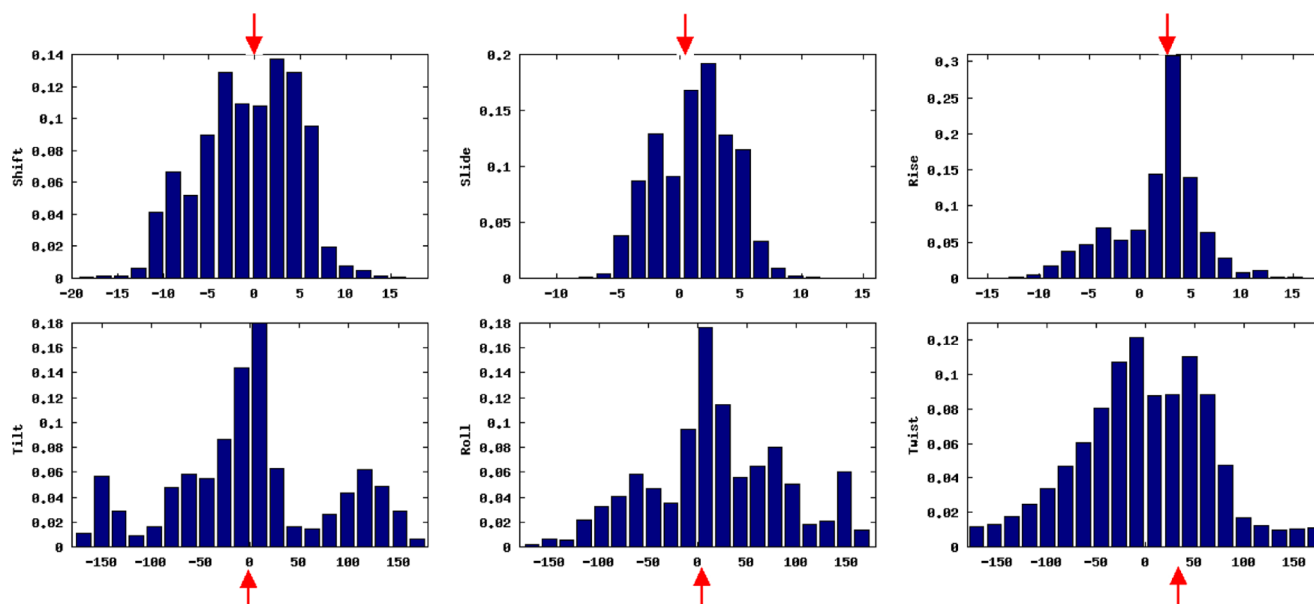


Figure 4. Distribution of the helical parameters of the single-stranded polyA at 350 K. The red arrows indicate the corresponding value for the ideal B-DNA helix.

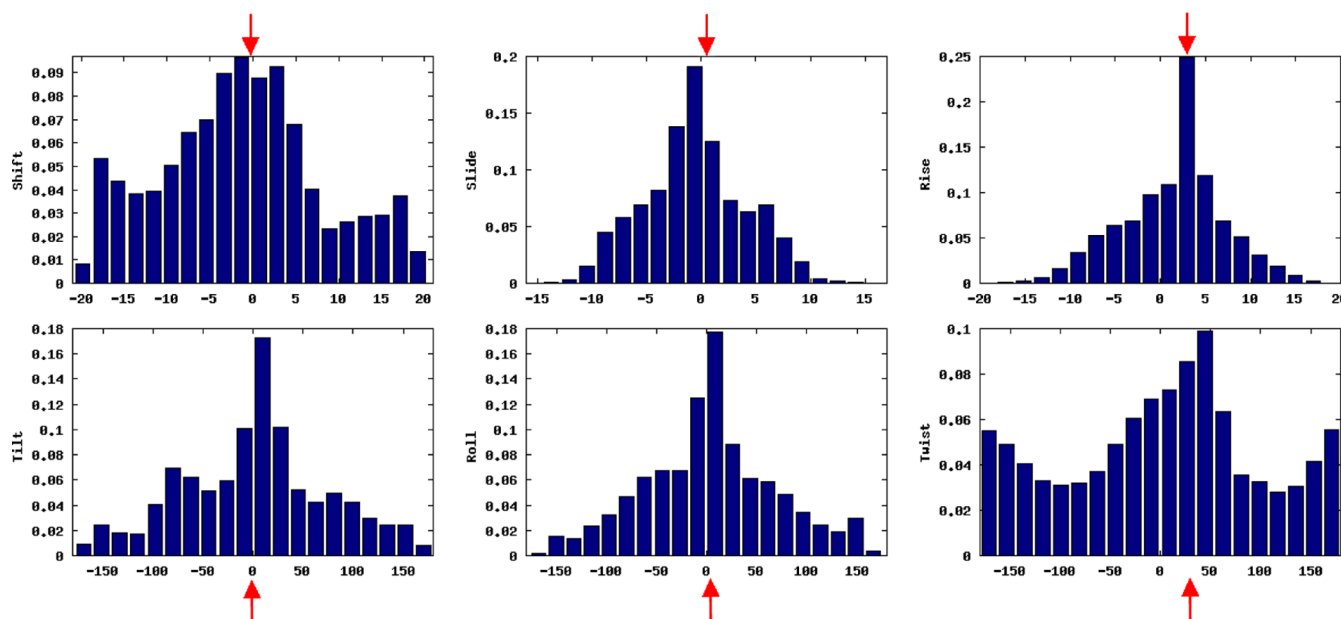


Figure 5. Distribution of the helical parameters of the single-stranded polyT at 350 K. The red arrows indicate the corresponding value for the ideal B-DNA helix.

helical parameters much broader than those observed in standard molecular dynamics simulations of ds-DNA,^{37,38} thus indicating the absence of conformational restraints due to the starting geometry (an ideal B-DNA helix). Such data, together with the relatively small error of the absorption spectra, indicate that the proposed explanation of the hyperchromic effect should not be affected by sampling issues.

CONCLUSIONS

Coupling high-level *ab initio* calculations of adenine and thymine and extended molecular dynamics simulations of DNA within a robust theoretical framework, as provided by the PMM procedure, the DNA electronic absorption spectra in single- and double-stranded conditions were calculated and compared

with the corresponding experimental signals. Our results point out that the well-known hyperchromic effect occurring in DNA is mainly due to the feature of the excitonic states, which are more delocalized in the single-stranded conditions, at least in the frequency window of the absorption maximum. Such states show an enhanced absorbance (with respect to the more localized states present in the double-stranded conditions), thus resulting in an absorbance increase of 28%, well reproducing the experimental data. In summary, the theoretical–computational procedure presented in this work was able to accurately reproduce the essential features of the DNA electronic absorption and to explain the DNA hyperchromism in terms of excitonic coupling among the nucleobases. Although care must be taken when using the excitonic theory because charge-

transfer states are not included, the accuracy of our theoretical–computational results in reproducing the main feature of the experimental signal of solvated DNA molecules indicates that when charge-transfer states have a negligible or even a limited effect on the absorption spectrum our methodology can represent a proper route for the characterization of the electronic behavior of complex systems involving interacting chromophores and delocalized excited states.

■ ASSOCIATED CONTENT

■ Supporting Information

Additional details on the computational results. This material is available free of charge via the Internet at <http://pubs.acs.org>.

■ AUTHOR INFORMATION

Corresponding Author

*E-mail: mdabramo.res@gmail.com (M.D.); a.amadei@uniroma2.it (A.A.).

Notes

The authors declare no competing financial interest.

■ REFERENCES

- (1) Merino, E.; Boal, A. Biological Contexts for DNA Charge Transport Chemistry. *Curr. Opin. Chem. Biol.* **2008**, *12*, 229–237.
- (2) Boal, A. K.; Genereux, J. C.; Sontz, P. A.; Gralnick, J. A.; Newman, D. K.; Barton, J. K. Redox Signaling between DNA Repair Proteins for Efficient Lesion Detection. *Proc. Natl. Acad. Sci. U.S.A.* **2009**, *106*, 15237–15242.
- (3) Tanaka, H.; Kawai, T. Partial Sequencing of a Single DNA Molecule with a Scanning Tunnelling Microscope. *Nat. Nanotechnol.* **2009**, *4*, 518–522.
- (4) Gonzalez-Bosquet, J.; Calcei, J.; Wei, J. S.; Garcia-Closas, M.; Sherman, M. E.; Hewitt, S.; Vockley, J.; Lissowska, J.; Yang, H. P.; Khan, J.; et al. Detection of Somatic Mutations by High-Resolution DNA Melting (HRM) Analysis in Multiple Cancers. *PLoS One* **2011**, *6*, e14522.
- (5) Galetto, R.; Duchateau, P.; Pâques, F. Targeted Approaches for Gene Therapy and the Emergence of Engineered Meganucleases. *Expert Opin. Biol. Ther.* **2009**, *9*, 1289–1303.
- (6) Crespo-Hernández, C. E.; Cohen, B.; Kohler, B. Base Stacking Controls Excited-State Dynamics in A.T DNA. *Nature* **2005**, *436*, 1141–1144.
- (7) Crespo-Hernández, C. E.; Cohen, B.; Hare, P. M.; Kohler, B. Ultrafast Excited-State Dynamics in Nucleic Acids. *Chem. Rev.* **2004**, *104*, 1977–2019.
- (8) Buchvarov, I.; Wang, Q.; Raytchev, M.; Trifonov, A.; Fiebig, T. Electronic Energy Delocalization and Dissipation in Single- And Double-Stranded DNA. *Proc. Natl. Acad. Sci. U.S.A.* **2007**, *104*, 4794–4797.
- (9) Su, C.; Middleton, C. T.; Kohler, B. Base-Stacking Disorder and Excited-State Dynamics in Single-Stranded Adenine Homo-oligonucleotides. *J. Phys. Chem. B* **2012**, *116*, 10266–10274.
- (10) Kadhane, U.; Holm, A. I. S.; Hoffmann, S. V.; Nielsen, S. B. Strong Coupling between Adenine Nucleobases in DNA Single Strands Revealed by Circular Dichroism Using Synchrotron Radiation. *Phys. Rev. E* **2008**, *77*, 021901.
- (11) Markovitsi, D.; Gustavsson, T.; Banyasz, A. Absorption of UV Radiation by DNA: Spatial and Temporal Features. *Mutat. Res.* **2010**, *704*, 21–28.
- (12) Santoro, F.; Barone, V.; Improta, R. Influence of Base Stacking on Excited-State Behavior of Polyadenine in Water, Based on Time-Dependent Density Functional Calculations. *Proc. Natl. Acad. Sci. U.S.A.* **2007**, *104*, 9931–9936.
- (13) Tonzani, S.; Schatz, G. C. Electronic Excitations and Spectra in Single-Stranded DNA. *J. Am. Chem. Soc.* **2008**, *130*, 7607–7612.
- (14) Shukla, M. K.; Leszczynski, J. Electronic Spectra, Excited State Structures and Interactions of Nucleic Acid Bases and Base Assemblies: A Review. *J. Biomol. Struct. Dyn.* **2007**, *25*, 93–118.
- (15) Nielsen, L. M.; Pedersen, S. O. v.; Kirketerp, M.-B. S.; Nielsen, S. B. n. Absorption by DNA Single Strands of Adenine Isolated in Vacuo: The Role of Multiple Chromophores. *J. Chem. Phys.* **2012**, *136*, 064302.
- (16) Bouvier, B.; Gustavsson, T.; Markovitsi, D.; Milliè, P. Dipolar Coupling between Electronic Transitions of the DNA Bases and Its Relevance to Exciton States in Double Helices. *Chem. Phys.* **2002**, *275*, 75–92.
- (17) Aschi, M.; Spezia, R.; Nola, A. D.; Amadei, A. a First-Principles Method to Model Perturbed Electronic Wavefunctions: The Effect of an External Homogeneous Electric Field. *Chem. Phys. Lett.* **2001**, *344*, 374–380.
- (18) Spezia, R.; Aschi, M.; Di Nola, A.; Amadei, A. Extension of the Perturbed Matrix Method: Application to a Water Molecule. *Chem. Phys. Lett.* **2002**, *365*, 450–456.
- (19) Amadei, A.; D'Alessandro, M.; D'Abramo, M.; Aschi, M. Theoretical Characterization of Electronic States in Interacting Chemical Systems. *J. Chem. Phys.* **2009**, *130*, 084109.
- (20) Emanuele, E.; Markovitsi, D.; Milliè, P.; Zakrzewska, K. UV Spectra and Excitation Delocalization in DNA: Influence of the Spectral Width. *ChemPhysChem* **2005**, *6*, 1387–1392.
- (21) Amadei, A.; Daidone, I.; Aschi, M. a General Theoretical Model for Electron Transfer Reactions in Complex Systems. *Phys. Chem. Chem. Phys.* **2012**, *14*, 1360–1370.
- (22) Lu, X.-J.; Olson, W. K. 3DNA: A Versatile, Integrated Software System for the Analysis, Rebuilding and Visualization of Three-Dimensional Nucleic-Acid Structures. *Nat. Protoc.* **2008**, *3*, 1213–1227.
- (23) Perez, A.; Marchan, I.; Svozil, D.; Sponer, J.; T. E., C., III; Laughton, C. A.; Orozco, M. Refinement of the AMBER Force Field for Nucleic Acids: Improving the Description of Alpha/Gamma Conformers. *Biophys. J.* **2007**, *92*, 3817–3829.
- (24) Hess, B.; Kutzner, C.; van der Spoel, D.; Lindahl, E. GROMACS 4: Algorithms for Highly Efficient, Load-Balanced, and Scalable Molecular Simulation. *J. Chem. Theory Comput.* **2008**, *4*, 435–447.
- (25) Bussi, G.; Donadio, D.; Parrinello, M. Canonical Sampling through Velocity Rescaling. *J. Chem. Phys.* **2007**, *126*, 014101.
- (26) Parrinello, M.; Rahman, A. Polymorphic Transitions in Single Crystals: A New Molecular Dynamics Method. *J. Appl. Phys.* **1981**, *52*, 7182–7190.
- (27) Darden, T.; York, D.; Pedersen, L. Particle Mesh Ewald: An N [center-dot] log(N) method for Ewald Sums in Large Systems. *J. Chem. Phys.* **1993**, *98*, 10089–10092.
- (28) Werner, H.-J.; Knowles, P. J.; Knizia, G.; Manby, F. R.; Schütz, M. Molpro: A General Purpose Quantum Chemistry Program Package. *Wiley Interdiscip. Rev.: Comput. Mol. Sci.* **2012**, *2*, 242–253.
- (29) Werner, H.-J.; Knowles, P. J. A Second Order MCSCF Method with Optimum Convergence. *J. Chem. Phys.* **1985**, *82*, 5053.
- (30) Knowles, P. J.; Werner, H.-J. An Efficient Second Order MCSCF Method for Long Configuration Expansions. *Chem. Phys. Lett.* **1985**, *115*, 259–267.
- (31) Werner, H.-J. Third-Order Multiconfiguration Reference Perturbation Theory: The CASPT3Method. *Mol. Phys.* **1996**, *89*, 645–661.
- (32) Shiozaki, T.; G., W.; Celani, P.; Werner, H.-J. Communication: Extended Multi-State Complete Active Space Second-Order Perturbation Theory: Energy and Nuclear Gradients. *J. Chem. Phys.* **2011**, *135*, 081106.
- (33) Ghigo, G.; Roos, B. O.; Malmqvist, P. a Modified Definition of the Zeroth-Order Hamiltonian in Multiconfigurational Perturbation Theory (CASPT2). *Chem. Phys. Lett.* **2004**, *396*, 142–149.
- (34) D'Abramo, M.; Orozco, M.; Amadei, A. Effects of Local Electric Fields on the Redox Free Energy of Single Stranded DNA. *Chem. Commun.* **2011**, *47*, 2646–2648.
- (35) D'Abramo, M.; Di Nola, A.; Aschi, M.; Amadei, A. Theoretical Characterization of Temperature and Density Dependence of Liquid

Water Electronic Excitation Energy: Comparison with Recent Experimental Data. *J. Chem. Phys.* **2008**, *128*, 021103.

(36) D'Abramo, M.; Aschi, M.; Amadei, A. Charge Transfer Equilibria of Aqueous Single Stranded DNA. *Phys. Chem. Chem. Phys.* **2009**, *11*, 10614–10618.

(37) Dans, P. D.; Pérez, A.; Faustino, I.; Lavery, R.; Orozco, M. Exploring Polymorphisms in B-DNA Helical Conformations. *Nucleic Acids Res.* **2012**, *40*, 10668–10678.

(38) Lavery, R.; et al. A Systematic Molecular Dynamics Study of Nearest-Neighbor Effects on Base Pair and Base Pair Step Conformations and Fluctuations in B-DNA. *Nucleic Acids Res.* **2010**, *38*, 299–313.